THE AMERICAN SOCIETY OF MECHANICAL ENGINEERS
345 E. 47 St., New York, N.Y. 10017

92-GT-280

Cold Flow Testing of the Space Shuttle Main Engine Alternate Turbopump Development High Pressure Fuel Turbine Model

STEPHEN W. GADDIS and SUSAN T. HUDSON
NASA-Marshall Space Flight Center
Structure and Dynamics Lab, Experimental Branch
Huntsville, AL 35812

P. DEAN JOHNSON
Pratt and Whitney
Turbine Aerodynamics
West Palm Beach, FL 33410

ABSTRACT

The National Aeronautics and Space Administration's (NASA's) Marshall Space Flight Center (MSFC) has established a "cold" airflow turbine test program to experimentally determine the performance of liquid rocket engine turbopump drive turbines. Testing of the space shuttle main engine (SSME) alternate turbopump development (ATD) fuel turbine was conducted for "back-to-back" comparisons with the baseline SSME fuel turbine results obtained in the first quarter of 1991. Turbine performance, Reynolds number effects, and turbine diagnostics, such as stage reactions and exit swirl angles, were investigated at the turbine design point and at off-design conditions. The test data showed that the ATD fuel turbine test article was approximately 1.4 percent higher in efficiency and flowed 5.3 percent more than the baseline fuel turbine test article. This paper describes the method and results used to validate the ATD fuel turbine aerodynamic design. The results are being used to determine the ATD high pressure fuel turbopump (HPFTP) turbine performance over its operating range, anchor the SSME ATD steady-state performance model, and validate various prediction and design analyses.

NOMENCLATURE

A_n	First vane gauge area
CP	Specific heat at constant pressure
D	Reference diameter
g	Conversion constant 32.174 (lbm-ft)/(lbf-s^2)
J	Conversion constant 778 ft-lbf/Btu
K	Conversion constant (2π rad/rev)/60 s/min)
L	Actual chord length
Ma	Axial mach number based on turbine conditions
N	Shaft rotational speed
P	Pressure
Pr	Total-to-total pressure ratio
R	Gas constant
Re	Reynolds number
SP	Speed parameter
T	Temperature
TDC	Top dead center
Tq	Torque
U	Disk tangential speed
V	Velocity
VR	Velocity ratio
W	Mass flow rate
γ	Ratio of specific heats
η	Efficiency
μ	Viscosity
ρ	Density

Subscripts

0	Total
1	Turbine inlet
2	Turbine outlet

INTRODUCTION

The SSME ATD HPFTP consists of a high pressure hydrogen pump driven by a two stage axial flow turbine. This turbine is a low-pressure ratio reaction turbine driven by a mixture of steam and gaseous hydrogen. The turbine produces approximately 73,000 hp (54,436 kW) with a blade tip diameter of only 10 in (25.64 cm). At its design point, the turbine operates with an inlet temperature of about 1,900 ^{o}R (1,056 K) and an inlet pressure of approximately 5,200 psi (35.8 MPa). In order to reduce dynamic stresses and increase durability, the ATD HPFTP turbine incorporates a 10-percent reduction in rotor diameter relative to the baseline HPFTP turbine. While this diameter reduction increases turbine aerodynamic loading, the ATD turbine is predicted to achieve baseline turbine performance levels and not disrupt the current engine balance. The requirement of maintaining the current engine balance, along with the difficulty in accurately measuring turbine performance at the prototype's harsh operating conditions, brought about the need to experimentally determine the ATD HPFTP turbine efficiency and flow characteristics. Therefore, NASA's MSFC has established a "cold" airflow turbine test program for liquid rocket engine turbines. The testing of the ATD fuel turbine was conducted for "back-to-back" comparisons with the baseline fuel turbine testing completed during the first quarter of 1991 (Hudson, et al., 1991). As in the baseline test, the ATD turbine test used scaled test conditions to predict the performance of the ATD prototype. This paper describes the method and the results used to validate the aerodynamic design of the ATD fuel turbine. The results of this test are being used to determine the ATD HPFTP turbine performance over its operating range, anchor the SSME ATD steady-state performance model (power balance model), and validate various prediction and design codes.

Presented at the International Gas Turbine and Aeroengine Congress and Exposition
Cologne, Germany June 1-4, 1992

FACILITY DESCRIPTION

The test was conducted in the MSFC airflow turbine test equipment (TTE) as shown in Fig. 1. The TTE is a blowdown facility which operates by expanding high pressure air from one or two 6,000 ft^3 (170 m^3) air tanks at 420 psig (2.9 MPa) to atmospheric conditions. Air flows from the storage tanks through a heater section, quiet trim control valve, calibrated subsonic mass flow venturi, and into a plenum section. The air then passes through the test model and exhausts to atmosphere. This equipment can deliver 220 psia (1.5 MPa) air for run times from 30 s to over 5 min. The heater allows a blowdown controlled temperature between 530 ^oR (294 K) and 830 ^oR (461 K). The TTE has manual set point closed-loop control of the model inlet total pressure, inlet total temperature, shaft rotational speed, and pressure ratio. In addition to these control parameters, the facility can accurately measure mass flow, torque, and horsepower. Facility instrumentation also allows the measuring of 400 pressures, 120 temperatures, and various health monitoring variables. A more detailed description of the TTE design has been presented by Carter (1991). A description of its performance, time histories, and measurement uncertainties is given by Kauffman, et al. (1992).

MODEL DESCRIPTION

The model tested, named the ATD HPFTF turbine test article (TTA), is a full-scale model of the Pratt and Whitney ATD HPFTP turbine (Fig. 2). The mean line airfoil diameter was 9.150 (23.24 cm) and the first stage vane gauge area was 9.549 in^2 (61.61 cm^2). The inlet dome/strut assembly, stators, and rotors accurately duplicated the ATD HPFTP turbine gas path geometry by utilizing engine hardware fitted and instrumented in the model casings within engine tolerances. The model inlet flow was axially fed into the turbine with zero swirl. The SSME turbine exit circumferential pressure gradient, disk coolant flows, and blade platform seal leakages were not simulated. The rotor tip and gas path seal clearances represented nominal engine clearances. The model exhausted axially into a collector which served to direct the flow radially downward and diffused the flow to minimize the circumferential pressure gradient at the TTA exit. This test was designed to evaluate uncooled turbine performance; as such, all internal coolant leakage paths were sealed, with the exception of small well-defined ventilating flows to prevent disk cavity heating.

INSTRUMENTATION

The TTA was instrumented for two purposes: (1) aerodynamic measurements to calculate turbine performance and loads; (2) model health monitoring measurements to ensure the safe operation of the model.

Figure 3 gives an overview of the model instrumentation. The turbine inlet plane had stationary rakes, while the exit plane was defined by an instrumented ring which could rotate 90° about the model centerline. Both planes contained four total pressure and four total temperature rakes positioned 90° apart. Each rake had five radial kielhead probes at centers of equal area. The inlet rake kielheads were pitched to align with the inlet flow around the inlet dome. The inlet rakes were fixed in the yaw direction, but the exit rakes were manually adjusted for different levels of swirl. Two autonulling cobra probes were mounted on the exit ring. The cobra probes were positioned 180° apart and were mounted on radial traverse actuators. This allowed radial surveys of pressure, temperatures, and flow angle to be made at various circumferential locations. An estimate of instrumentation blockage effects on efficiency measurement was less than 0.04 percent and therefore neglected.

Model diagnostic instrumentation consisted of static pressure measurements throughout the turbine rows. There were eight equally spaced (circumferentially) static pressure taps on the annulus outer and inner diameters at eight axial planes. Also included were disk cavity gas pressures and temperatures along with the facility measurements mentioned previously in the "Facility Description." The health monitoring and special purpose instrumentation included tip clearance probes, bearing outer race metal temperatures, speed pickups, accelerometers, and casing metal temperatures.

TEST MATRIX

Similar to the baseline HPFTP TTA test, the testing of the ATD HPFTP TTA was conducted at "cold air" equivalent conditions in three parts (Table 1). Part A was dedicated to testing the model at the SSME 104-percent (design point, N = 6,982 r/m and Pr = 1.463) and 65-percent power levels. Set point accuracy, measurement repeatability, and Reynolds number effects were investigated. Also, TTA exit flow field parameters (pressure, temperature, and flow angle) were mapped radially and circumferentially. Part B assessed the turbine performance over the entire engine operating range from the 65-percent to the 109-percent power level. The turbine performance at extreme off-design conditions was investigated in part C. After facility inlet conditions achieved steady-state, 10 data scans were taken at 10-s intervals per run (or blowdown) at a constant set point and then numerically averaged.

DATA REDUCTION

Data reduction consisted of two phases: (1) on-line calculations and (2) off-line calculations, plots, and detailed analyses. On-line data calculations were performed immediately following the data acquisition process and were used to assess whether the run just completed was acceptable. The calculations consisted of measurement averages and key overall performance parameters for each scan of data. Off-line calculations and plotting were done on three levels:

(1) Plotting of raw data versus span, circumference, and axial location.

(2) Plotting of averaged data and comparison of overall turbine performance to predictions for a given run.

(3) Analysis of run-to-run data, comparison to predictions, and plotting of turbine performance curves.

RESULTS AND DISCUSSION

Radial and Circumferential

A survey of the exit flow field during test part A revealed a circumferential variation in the measured exit temperature. This variation occurred at an interval equal to the second vane pitch (6.67°) and caused a 1 to 2 point variation in calculated turbine efficiency. The variation was first discovered by rotating the exit rakes over an 18° arc in 2° increments, covering 3-s vane pitches per exit rake. Pressure and temperature measurements were averaged in order to provide a more representative measurement of the exit flow

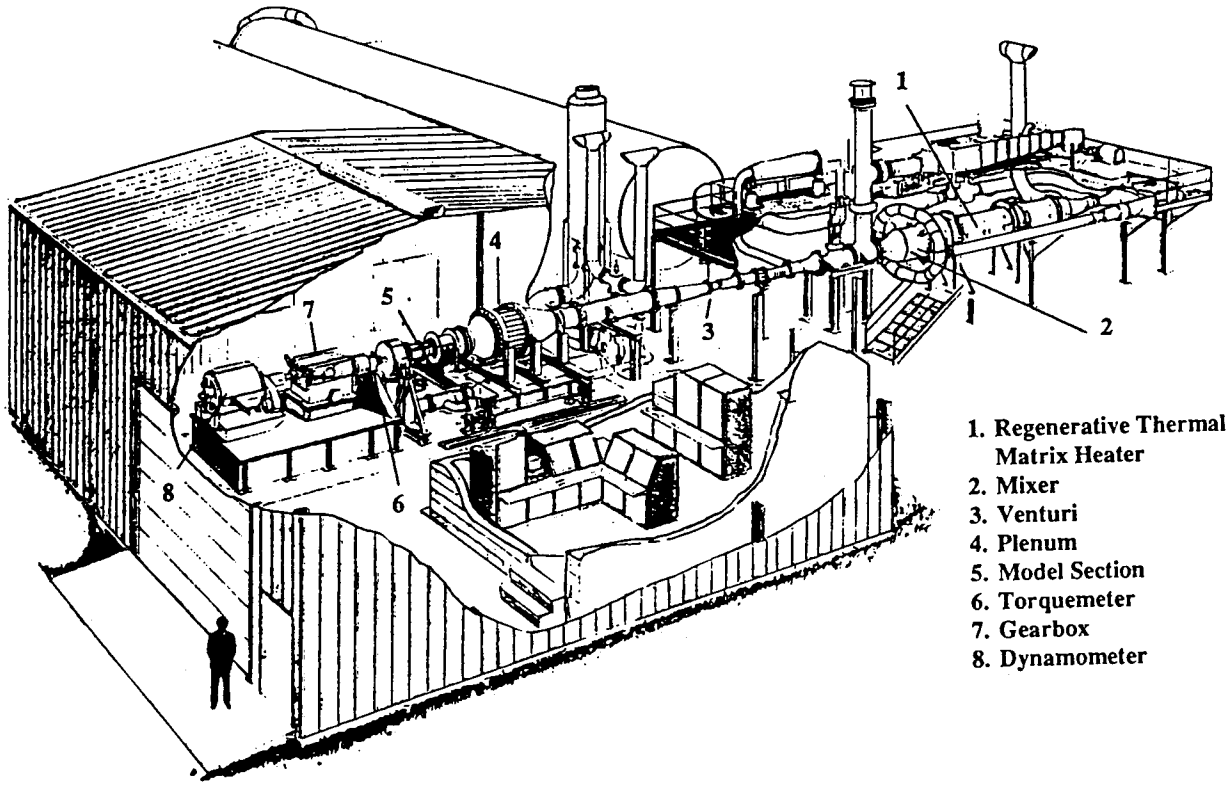

FIG. 1 SCHEMATIC OF TTE

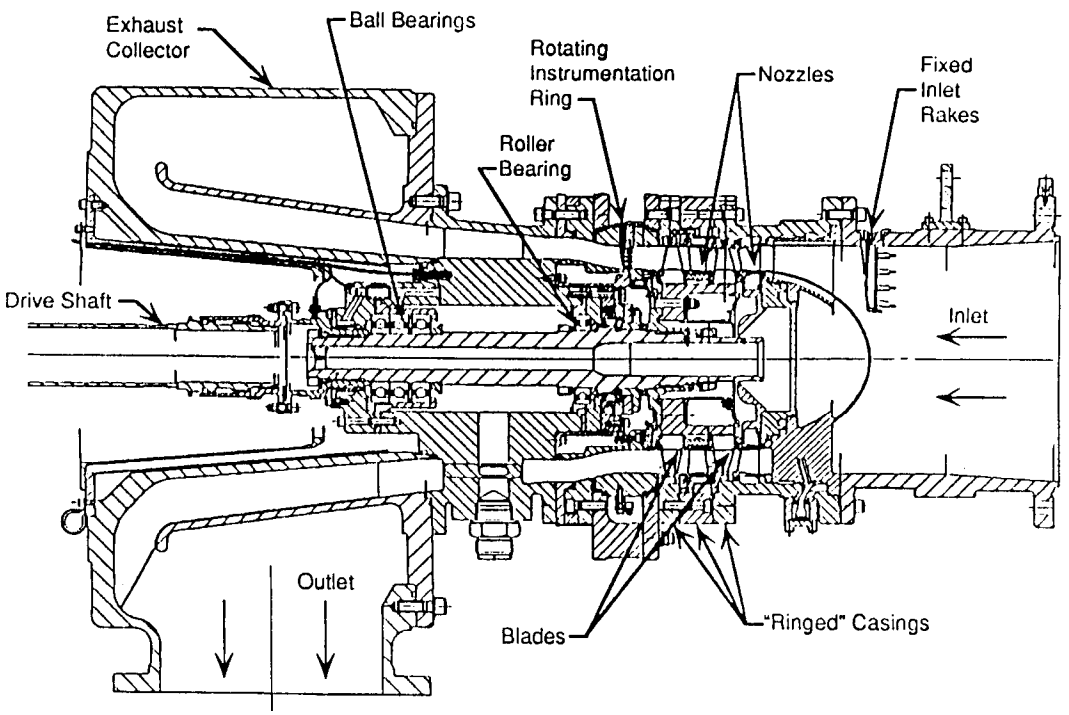

FIG. 2 CROSS SECTION OF TTA

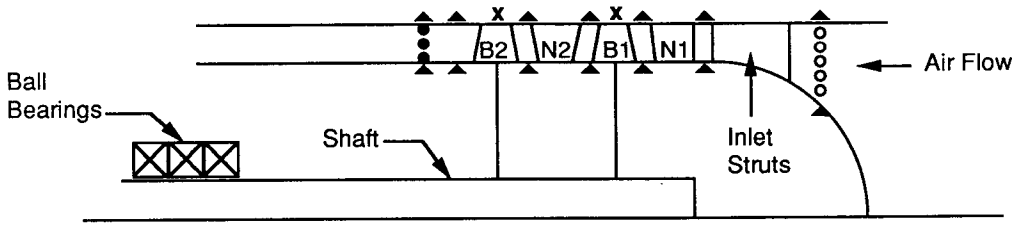

X Tip Clearance Probes (3 Circumferential)
▲ Gas Path Wall Static Pressures (8 Circumferential)
● Exit Rotating Ring (Continuously Variable Through 90 Deg.)
-8 Equally Spaced Rakes (Circumferential)
-4 Total Temperature With 5 Radial Sensors
-4 Total Pressure With 5 Radial Sensors
o Fixed Inlet Rakes (8 Circumferential)
-4 Total Temperature With 5 Radial Sensors
-4 Total Pressure With 5 Radial Sensors
N1 First Stage Nozzle
B1 First Stage Rotor
N2 Second Stage Nozzle
B2 Second Stage Rotor

FIG. 3 ATD TTA PHASE I PERFORMANCE INSTRUMENTATION OVERVIEW

TABLE 1 PHASE I TEST MATRIX

Test Part	Objective	Set Point Conditions	Model Conditions at Turbine Exit
A	Design point performance, assess Re effects, and survey turbine exit flowfield	To=550°R (306°K) Po=27(186),35(241), 50(345),75(517),100(689), 125(861),150(1034),175 (1206),200(1378) psia(kPa) N=6982,5520 RPM	Re=316,938-2,519,990 Ma=0.15-0.19 Flow angle=+7-+14
B	Map 65% to 109% RPL performance and survey turbine exit flowfield at matrix corners.	To=550° R, Po=100 psia Pr=1.30,1.35,1.40, 1.45,1.463,1.50 N=5000,5500,6000, 6500,6982,7500 RPM	Re=1,116,028-1,427,819 Ma=0.14-0.28 Flow angle=-20-+30
C	Map extreme off-design point performance	To=550° R Po=100 psia, Pr=1.20, 1.30,1.40,1.50,1.60 N=2000,4000,5000, 6000,8000,10000 RPM	Re=958,142-1,638,488 Ma=0.12-0.48 Flow angle=-28-+49

field. This system of mapping the exit flow field, clocking 18° in 2° increments, was employed throughout the test program. A full 360° circumferential mapping of the exit flow field validated that the 18° per rake mapping gave an accurate measurement of the exit temperature and pressure. Figure 4 shows the exit temperature contour for the design point from 15- to 90-percent span over 360°. (Note: rotation was clockwise looking upstream). Higher temperature regions were present near the outer diameter (OD) of the flow path resulting from less efficient tip clearance and endwall regions of the turbine rotors. The exit temperature contour also showed circumferential periodicity that occurred at an interval equal to the second stage vane wakes. The exit pressure contour was investigated in the same manner as the exit temperature contour. The pressure contour varied only 1 psia (6.89 kPa) spanwise, and showed no variation circumferentially (Fig. 5).

The two exit cobra probes were used to investigate flow near the hub and tip end walls. Measurements were collected at 10 spanwise locations from 5- to 100-percent span. Data was taken over an 8° circumferential traverse. Figure 6 shows the cobra probe temperature data for one blade pitch. The cobra probe data revealed no temperature or pressure spikes near the end-wall region, and validated the measurements taken with the exit temperature and pressure rakes.

The cobra probes were also used to map the spanwise and circumferential variations in exit swirl (positive swirl in the counterclockwise direction looking upstream), see Fig. 7 for one blade pitch. The swirl angles varied 30° from hub to tip, but showed almost no variation circumferentially. The midspan position was found to be a representation average for the spanwise swirl. Therefore, after mapping the swirl for part A,

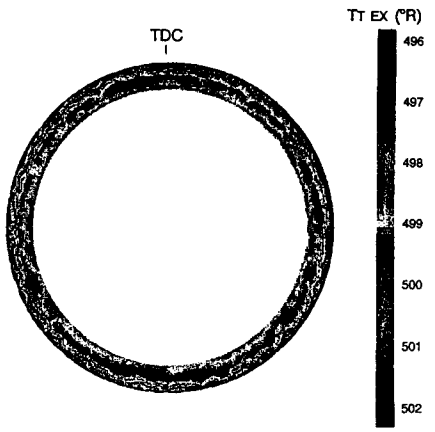

FIG. 4 EXIT TEMPERATURE PROFILE AT DESIGN POINT (view is aft looking upstream)

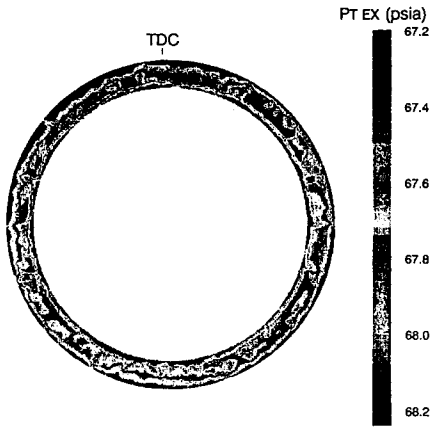

FIG. 5 EXIT PRESSURE PROFILE AT DESIGN POINT (view is aft looking upstream)

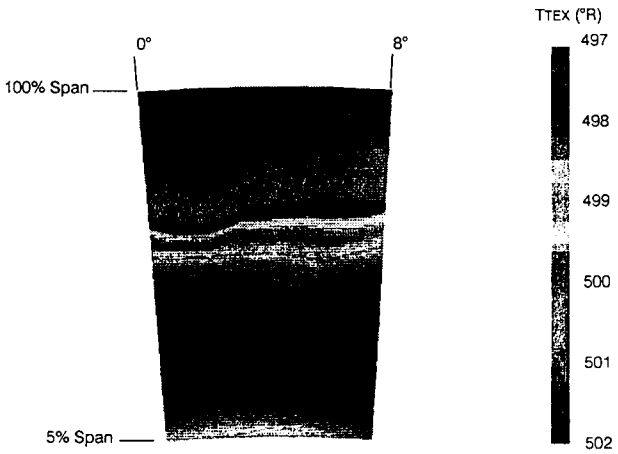

FIG. 6 COBRA PROBE EXIT TEMPERATURE AT 104-PERCENT RPL

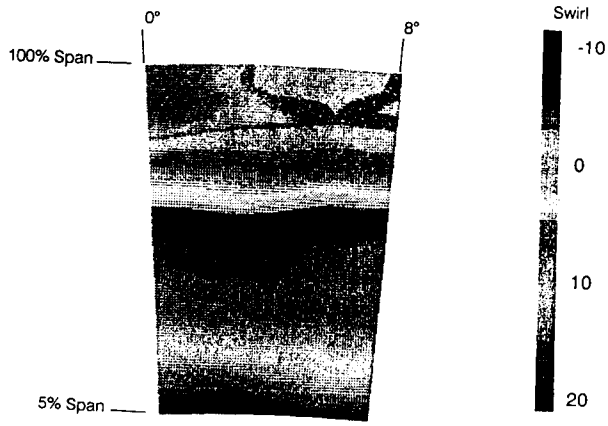

FIG. 7 COBRA PROBE EXIT SWIRL ANGLE AT 104-PERCENT RPL

the swirl angle was only measured at midspan for parts B and C (Fig. 8).

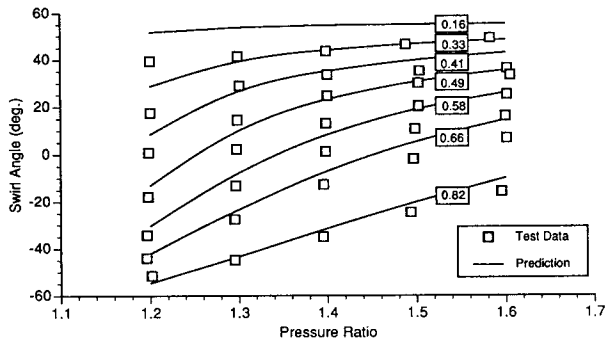

FIG. 8 TURBINE EXIT SWIRL ANGLE VERSUS PRESSURE RATIO FOR THE ATD MODEL WITH CONSTANT LINES OF SPEED PARAMETER

Reynolds Number Effects

Testing in the TTE was based on the principle of similitude. The following functional relationship for mass flow and efficiency was used (Horlock, 1966):

$$\frac{W\sqrt{RT_{01}}}{P_{01}A_n},\ \eta = f\left(\frac{ND}{\sqrt{RT_{01}}},\ \frac{P_{01}}{P_{02}},\ \frac{W}{\mu D},\ \gamma\right), \quad (1)$$

where:

$\frac{W\sqrt{RT_{01}}}{P_{01}A_n}$ = flow parameter

$\frac{ND}{\sqrt{RT_{01}}}$ = speed parameter

or

$\frac{U}{\sqrt{2CpT_{01}\left[1-\left(\frac{P_{02}}{P_{01}}\right)^{\frac{\gamma-1}{\gamma}}\right]}}$ = velocity ratio

$\frac{P_{01}}{P_{02}}$ = pressure ratio

$\frac{W}{\mu D}$ = Re based on mass flow .

The speed parameter can be rewritten as velocity ratio (U/Co). This equation was utilized to establish the model set point conditions for the facility. Setting the facility inlet temperature (T_{01}), inlet pressure (P_{01}), pressure ratio across the model (Pr), and the

model shaft speed (N) fixed the speed parameter, pressure ratio, and Reynolds number and also established a corresponding engine power level.

In similar airflow turbine testing, the Reynolds number and ratio of specific heats are often considered insignificant and dropped from Eq. (1). Knowing the effects of the ratio of specific heats are negligible for simple compressible flow at low mach numbers, they were considered negligible here as well. The Re effects were investigated since accuracies of 1 percent or less were targeted for this test and the model and prototype Reynolds numbers differed by an order of magnitude. The operational Re used was an average of the first stator exit Re and the second rotor exit Re. This definition associated Re with the appropriated loss mechanism, airfoil profile losses, which characterized the turbine better than an overall number based on mass flow. The Reynolds number for ATD testing was defined as follows:

$$Re = \frac{rVL}{\mu}, \qquad (2)$$

with the gas properties evaluated at the first stator exit and the second rotor exit. The reference velocities were airfoil exit relative values and the characteristic dimension (L) was airfoil axial chord. Runs were made to study the Re effects at both the 104-percent and the 65-percent power levels. Inlet total pressure was varied to change the Re at each power level. A comparison between the 104-percent Re data and the pretest prediction is given in Fig. 9. The following turbulent boundary layer Reynolds number prediction (Glassman, 1972) was used:

$$\left\{\frac{1-\eta_{design}}{1-\eta}\right\} = \left\{\frac{Re}{Re_{design}}\right\}^{0.042}. \qquad (3)$$

The value of the exponent was derived beyond its original bounds by previous engine test data. This correlation was used to extrapolate between the test Re and the engine Re. The data matches the prediction well at Reynolds numbers of approximately one million and above. This corresponds to inlet total pressures of 75 psia (517 kPa) and above. At inlet pressures of 75 psia and below, the data did not match the prediction. The reasons for this deviation from the prediction are not fully understood. The 65-percent power level results were similar to the 104-percent power level results. It was concluded that Re effects were small, but they were measurable and quantifiable. For the remainder of phase I testing, the inlet total pressure was set to 100 psia (689 kPa). Speed and pressure ratio were varied to set the operating conditions for parts B and C.

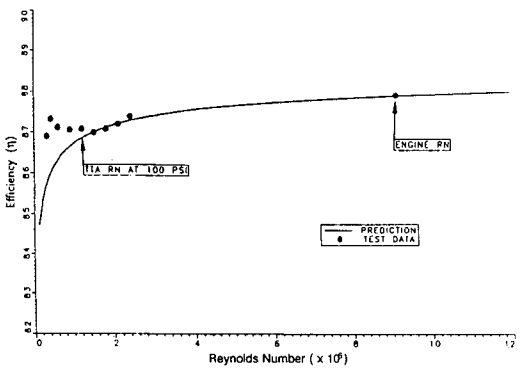

FIG. 9 EFFICIENCY VERSUS REYNOLDS NUMBER AT 104-PERCENT POWER LEVEL

Tip Clearance

Three equally spaced tip clearance probes were used per stage. The tip clearance was measured for varying speed, inlet total pressure, and pressure ratio. No changes in tip clearance were observed for varying pressure ratio and inlet pressure. Over most of the operating speed range (0 to 8,000 r/min), the tip clearance remained at the build clearances of 0.017 in (0.044 cm) and 0.014 in (0.036 cm) for the first and second rotors, respectively. However, at 10,000 r/min the tip clearance decreased approximately 0.002 in (0.005 cm) to 0.004 in (0.010 cm).

Static Pressures

Static pressures were measured on the annulus outer and inner diameters at eight axial locations (Fig. 3). The static pressure drop for seven axial locations through the turbine is presented in Fig. 10 for the design point. In Fig. 10, the average of the inner and outer diameter pressures is shown normalized by the inlet total pressure, and is shown plotted with mean line and three-dimensional (3-D) Euler predictions. Both codes predicted the design point static pressure drops within 2 percent. The inner and outer diameter static pressures were also compared to the 3-D Euler code predictions at the design point (Fig. 11). The hub and tip static pressures were accurately predicted within 1.5 percent. Mean line predictions were compared to the remaining test conditions. The predictions were more accurate (within 1 percent) at the higher velocity ratios than at the lower velocity ratios (within 6 percent).

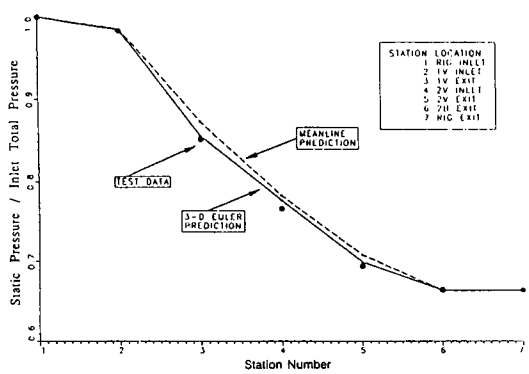

FIG. 10 STATIC PRESSURE DROP THROUGH TURBINE WITH MEAN LINE AND 3-D EULER PREDICTIONS

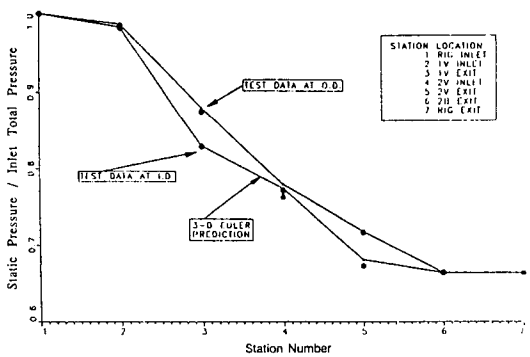

FIG. 11 INNER AND OUTER DIAMETER STATIC PRESSURE MEASUREMENTS WITH 3-D EULER PREDICTION

Overall Performance

Efficiency and flow parameter were used to quantify the overall turbine performance. Comparisons between the two turbines were made at the projected operating points (different speeds and pressure ratios), and not at the same VR. The efficiency was calculated by two different methods: the torque/mass (mechanical) method and the temperature difference (thermodynamic) method. The equations used to calculate efficiency were:

$$\eta = \frac{KTqN}{JC_pWT_{01}\left[1-\left(\frac{1}{Pr}\right)^{\frac{g-1}{g}}\right]}, \quad (4)$$

$$\eta = \frac{T_{01}-T_{02}}{T_{01}\left[1-\left(\frac{1}{Pr}\right)^{\frac{g-1}{g}}\right]}. \quad (5)$$

The torque used to calculate efficiency in Eq. (4) (leave out constant, J, for metric version) was corrected for rig mechanical losses and for aerodynamic disk windage losses. A previous test quantified the bearings and seals losses, but an analytical prediction was used to determine the disk windage losses.

The design point torque based efficiency was 85.3 percent compared to the temperature based efficiency of 87.2 percent. The temperature based efficiency was consistently 1.7 to 2.0 percent higher than the torque corrected efficiency. Inaccurate estimates of the rig windage and mechanical losses were believed to cause the difference in efficiencies. Both calculated efficiencies were compared to the mean line prediction in Fig. 12. The prediction matched both efficiencies within 1.4 percent at design and within 4.0 percent over the entire test matrix. The test data showed that the ATD TTA operated at approximately 1.4 percent higher efficiency (temperature based) than the baseline TTA (Fig. 13).

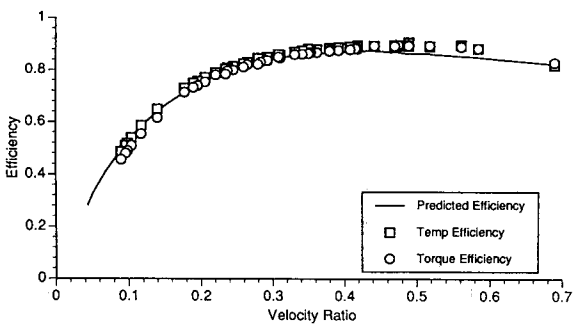

FIG. 12 EFFICIENCY VERSUS VELOCITY RATIO WITH MEAN LINE PRETEST PREDICTION

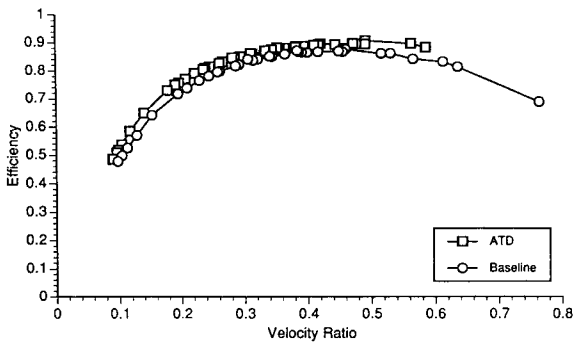

FIG. 13 COMPARISON OF ATD AND BASELINE TEMPERATURE EFFICIENCY VERSUS VELOCITY RATIO

The flow parameter at the design point was 0.47. Figure 14 showed the flow parameter versus speed parameter for lines of constant pressure ratio with the pretest mean line prediction. The prediction matched the test data at design within 4.5 percent and within 6.5 percent over the entire test matrix. The test data showed that the ATD TTA had a 4.6 percent higher flow parameter than the baseline TTA (Fig. 15) which translated to a 5.3 percent increase in flow due to differences in flow area.

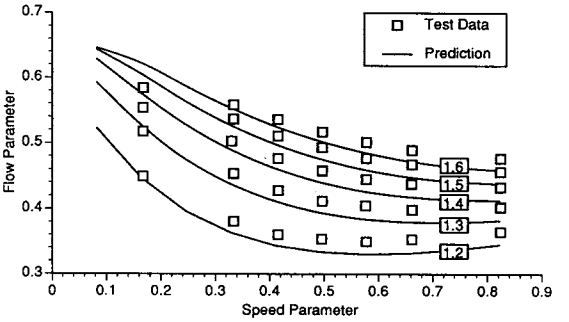

FIG. 14 FLOW PARAMETER VERSUS SPEED PARAMETER WITH PRETEST PREDICTION FOR CONSTANT LINES OF PRESSURE RATIO

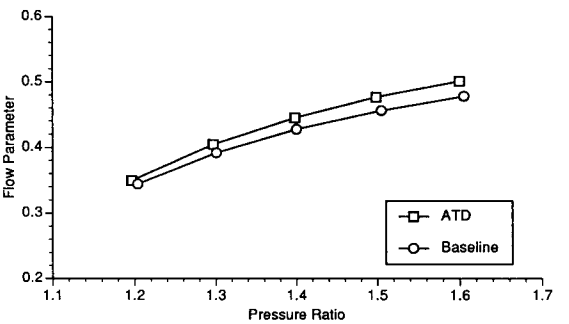

FIG. 15 COMPARISON OF ATD AND BASELINE FLOW PARAMETER VERSUS PRESSURE RATIO AT 7,000 RPM

UNCERTAINTY ANALYSIS

A posttest detailed uncertainty analysis of phase I data was performed according to ANSI/ASME performance test code (PTC) 19.1-1985 and Coleman and Steele (1989). The test data were scrutinized to establish the worst case uncertainties of the measured quantities. The analysis accounted for both bias and precision errors and were combined using the root sum square (RSS) method. The uncertainties were calculated for a 95-percent confidence level. The uncertainty calculated for thermodynamic efficiency at the design point was within 0.8 percent. In addition, the uncertainties calculated for the off-design runs were within 0.8 percent except for two conditions. The high- and low-velocity ratios for low-pressure ratio had uncertainties within 1.8 and 1.2 percent, respectively.

CONCLUSIONS

The phase I ATD turbine test established a data base for the SSME ATD HPFTP turbine at the design point and at off-design conditions. The test data provide an

accurate cold flow evaluation of the turbine performance. The turbine exit flow field has been thoroughly mapped and Reynolds number effects have been quantified. The data have been compared to pretest cold flow mean line predictions with good results. The test results showed that the SSME ATD HPFTP TTA operated at approximately 1.4 percent higher efficiency (temperature based), and flowed 5.3 percent more than the baseline SSME HPFTP TTA. The results are being scaled from cold flow conditions to engine conditions to assess the performance of the ATD HPFTP turbine at the SSME. The test results will also be used to improve mean line prediction codes, validate 3-D aerodynamic solvers, and improve the SSME ATD steady-state performance model (power balance model).

ACKNOWLEDGMENTS

The authors would like to thank Al Finke for running the test from day to day, John Heaman for maintaining the data acquisition systems, and Gary McGriff for operating the facility day in and day out. We would also like to thank the many others from NASA/MSFC, Pratt & Whitney, Microcraft, Inc., and Rotodata, Ltd., who helped make this project a success.

REFERENCES

Carter, J. A.: "Blowdown Turbine Test Equipment Design Characteristics," NASA/MSFC Memo ED35-45-91, 1991.

Kauffman, W. J., Jr., Carter, J. A., Heaman, J. P., and Bordelon, W. J., Jr.: "The Design and Performance of the Marshall Space Flight Center Turbine Test Equipment," (current conference paper), 1992.

Coleman, H. W., Steele, W. G., Jr.: Experimentation and Uncertainty Analysis for Engineers, John Wiley and Sons, Inc., 1989.

Gaddis, S. W.: "SSME Alternate Turbopump Development Turbine Test Article Phase I Pretest Report," NASA/MSFC Memo ED35-16-91, 1991.

Glassman, A. J.: Turbine Design and Application, vol. 1, NASA SP-290, 1972.

Horlock, J. H.: Axial Flow Turbines, Krieger Publishing Company, Malabar, FL, 1966.

Hudson, S. T., Gaddis, S. W., and Johnson, P. D.: "Cold Flow Testing of the Space Shuttle Main Engine High Pressure Fuel Turbine Model," AIAA Paper No. 91-2503, 1991.